

BEHAVIOR OF BUBBLES IN WELD UNDER MICROGRAVITY

K. NOGI¹†, Y. AOKI¹, H. FUJII¹ and K. NAKATA¹

¹Joining and Welding Research Institute, Osaka University, Mihogaoka, Ibaraki, Osaka 567-0047, Japan and ²Department of Materials Science and Processing, Faculty of Engineering, Osaka University, Yamadaoka, Suita, Osaka 565-0871, Japan

(Received 10 September 1997; accepted 8 February 1998)

Abstract—In order to investigate the effect of gravity on the behavior of bubbles in a weld, gas tungsten arc (GTA) welding was performed with an argon–1% hydrogen mixed shielding gas both in a microgravity environment and in a terrestrial environment. The microgravity environment was produced for 10 s with less than 10^{-5} G by a drop-shaft type microgravity system. The material used was an aluminum alloy. By classifying pores into blowholes and wormholes with the shape factor of pores and comparing the results in both environments, the following points have been found. In a terrestrial environment, bubbles smaller than 135 μm were not significantly affected by gravity. Larger bubbles move to the upper part of the molten metal due to buoyancy before the weld is solidified, but they scarcely combine together during the movement. In a microgravity environment, both blowholes and wormholes are distributed uniformly in the weld. © 1998 Acta Metallurgica Inc. Published by Elsevier Science Ltd. All rights reserved.

1. INTRODUCTION

A welding experiment in a microgravity environment can be regarded as a fundamental experiment to establish a welding technique in space as well as to clarify the complicated welding phenomena on the ground due to gravity. Experiments in a microgravity environment were started in 1969 by the U.S.S.R. [1] and then in 1973 by the U.S.A. [2]. These experiments showed that welding can be performed in space. However, detailed information on the welding phenomena in a microgravity environment has not been published. The authors have also investigated the welding phenomena in a microgravity environment and have made clear the effect of gravity on the weld shape, the arc shape, and the microstructure [3].

Pores are known as a welding defect. They are formed when bubbles cannot be released from a weld pool and are captured by the surrounding solid during the solidification process. The pores affect the mechanical properties such as the tensile strength, the proof strength, and the elongation [4], of a weld. The bubbles in a microgravity environment are expected to behave differently from those in a terrestrial environment because the effect of buoyancy and sedimentation is negligible. However, the behavior of bubbles has scarcely been investigated. In a previous paper [3], the authors observed the pores in a butt weld in a microgravity environment. However, because the number of pores was small, detailed information on the pores (e.g. pore

distribution and pore shape) was not obtained. In this study, in order to clarify the behavior of bubbles, gas tungsten arc (GTA) welding with an argon–1% hydrogen mixed shielding gas was carried out using a drop-shaft type system at Japan Microgravity Center (JAMIC).

2. CAUSES OF BUBBLE FORMATION

Pores are known as a welding defect. They are formed when bubbles cannot be released from a weld pool and are captured by the surrounding solid during the solidification process. Bubbles in a molten metal are mainly formed due to the following causes [5–8]:

1. Release of dissolved gas in a molten metal due to the decrease in the solubility of the gas during the cooling process [5].
2. Chemical reactions in a molten metal [5].
3. Trapped gas between root faces [6].
4. Evaporation of alloying elements with a high vapor pressure [7].
5. Physical trapping of shielding gas [8].

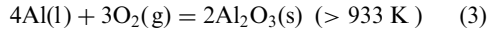
In aluminum alloys, hydrogen is a major cause of bubble formation [9]. However, in a vacuum condition such as in space, bubbles can be formed by another cause, too.

On the aluminum surface, an aluminum oxide always exists due to the following reactions [10]:



$$\Delta G^\circ = -3351510 + 629.85T \quad (\text{J/mol}) \quad (2)$$

†To whom all correspondence should be addressed.



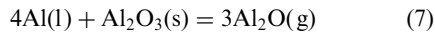
$$\Delta G^\circ = -3384270 + 662.88T \text{ (J/mol)} \quad (4)$$

where ΔG° is the change of standard free energy and T is temperature. However, when electron beam (EB) welding or laser beam (LB) welding is performed in a vacuum, the production of a gas (Al_2O) [10] becomes more important than in the atmosphere



$$\Delta G^\circ = -341410 - 98.74T \text{ (J/mol)}. \quad (6)$$

Therefore, the reaction between Al and Al_2O_3 which produces Al_2O is considered as follows:



$$\Delta G^\circ = 1180020 - 479.55T \text{ (J/mol)}. \quad (8)$$

Using these equations, the equilibrium Al_2O partial pressure is calculated as shown in Table 1. The Al_2O partial pressures are very high at higher temperatures. One of the authors has actually observed a reduction of the Al_2O_3 layer on the aluminum surface at 1373 K during an experiment [11].

In the LEO, atomic oxygen formed by the photodissociation of molecular oxygen is the most prevalent species [12]. Atomic oxygen oxidize a damaged part of space structures. When the damaged part is repaired, the reaction between Al and Al_2O_3 can occur, producing a gas phase of Al_2O . Thus, it is necessary to investigate the behavior of bubbles in space. In this study, because the GTA welding process was performed at an atmospheric pressure, an argon–1% hydrogen mixed shielding gas was used in order to simulate the behavior of bubbles in space.

3. EXPERIMENTAL

3.1. Experimental apparatus

Although microgravity environments can be achieved by several methods [13, 14], the drop-shaft microgravity system was used in this study. The system can maintain 10 s microgravity duration with a microgravity condition of less than 10^{-5} G. The quality of microgravity is the highest up to the present [15] and is similar to the space environment [3]. The drop capsule is composed of a

Table 1. Calculated partial pressure of Al_2O in equilibrium using the equation: $4\text{Al}(\text{l}) + \text{Al}_2\text{O}_3(\text{s}) = 3\text{Al}_2\text{O}(\text{g})$

Temperature, T (K)	$P_{\text{Al}_2\text{O}}$ (Pa)
1073	1.61×10^{-6}
1173	6.91×10^{-5}
1273	1.64×10^{-3}
1373	2.46×10^{-2}
1473	2.55×10^{-1}
1573	1.97

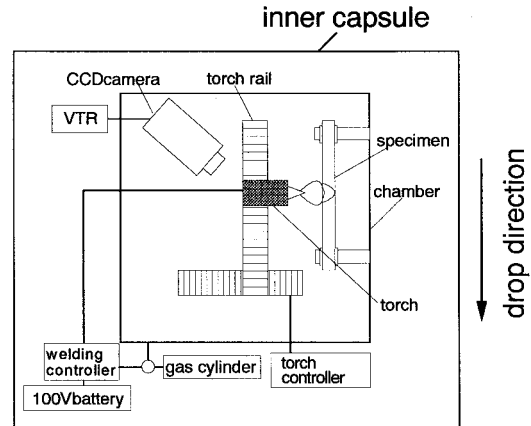


Fig. 1. Schematic illustration of GTA experimental apparatus.

double structure consisting of an inner and an outer capsule and a vacuum is maintained between them so that the free fall velocity of the GTA welding apparatus in the inner capsule will not be affected by the air drag. Figure 1 shows the GTA welding apparatus [3] used in this study. The apparatus consists of a welding chamber, a battery, a welding power source, a shielding gas supply, and a welding control system. The welding chamber is equipped with a specimen, a torch sliding system, and a CCD camera to observe the weld pool. The battery is an uninterruptible power system (UPS) which supplies 2.4 kW (AC100V, 3000VA) to the welding power source. The welding power source is a constant current type.

3.2. Experimental procedure

Tables 2 and 3 show the chemical composition of the aluminum alloy and the welding conditions, respectively. Bead-on-plate welding was performed and the welding position was horizontal. The polarity was the direct current electrode negative (DCEN). The flow rate of the shielding gas was optimized in a terrestrial environment and all specimens were welded with the same GTA welding apparatus. Note that an argon–1% hydrogen mixed gas was used as shielding gas in order to investigate the behavior of bubbles. Experiments were conducted both in a microgravity environment and in a terrestrial environment. Figure 2 shows a typical weld bead appearance of the microgravity experiments. Because it takes several seconds to obtain a stable arc and weld pool, even for the microgravity experiments the welding was performed in the terrestrial environment for the initial 20 s and then the

Table 2. Chemical composition of the aluminum alloy, mass%

Al	Mg	Mn	Fe	Cr	Si	Cu	Zn	Ti
Bal	4.41	0.62	0.21	0.12	0.09	0.02	0.02	0.02

Table 3. Welding conditions

Parameter	Conditions
Welding method	bead-on-plate welding
Sample size (mm ^l ×mm ^w ×mm ^t)	160 × 50 × 3
Shielding gas	argon-1% H ₂
Shielding gas flow rate (m ³ /s)	1.7 × 10 ⁻⁴
Welding position	horizontal
Welding current (A)	81
Welding voltage (V)	12
Welding velocity (m/s)	3.6 × 10 ⁻³

capsule was dropped to achieve a microgravity condition.

In order to investigate the weld shape and the distribution of pores, the welds were observed using a microscope after cutting, mechanical polishing, and electrical etching the specimens. Both pore size distribution and pore shape of the samples in both environments were measured from optical micrographs by image analysis on a Power Macintosh 7100/80AV computer. The resolution of the image analysis is about 3×10^{-6} m/pixel. In order to reduce statistical errors, five cross sections were selected and the values were averaged.

4. EXPERIMENTAL RESULTS

4.1. Distribution of pores in weld

Figure 3 shows transverse sections of the welds in both environments. The weld shape is significantly affected by gravity in the terrestrial environment, as illustrated in a previous paper [3]. It is also found that in the terrestrial environment, round shaped blowholes were segregated in the upper part. Wormholes were distributed only in the lower part of the weld. Figure 4 shows radiographs of the bead-on-plate weld in both environments. It is confirmed that the distributions of pores shown in Fig. 3 are observed from the beginning to the end of the welds. In the microgravity environments, on the other hand, blowholes and wormholes were distributed uniformly in the weld. The weld bead is formed more flatly in the microgravity environments than in the terrestrial environment though it is slightly bent due to the arc pressure [3].

In order to evaluate the pore size distribution quantitatively, image analyses were performed. Figure 5(a) shows the pore size distribution in the whole cross sections of both environments. Because the pore size distribution in both environments is not very different, it can be judged that the mechanism of the formation of bubbles is similar in both environments. However, the positions of pores are quite different. When the results in Fig. 5(a) are counted again separating the area into the upper and the lower parts, the results in Figs 5(b) and (c) are obtained. As shown in Fig. 5(c), pores are distributed uniformly in the weld of the microgravity condition. In the terrestrial environment, on the other hand, larger pores are mainly distributed in the upper part and more smaller pores are distributed in the lower part.

Therefore, it can be concluded that the bubbles are formed in a similar way in both environments but they are moved due to buoyancy only in the terrestrial environment.

4.2. Pore shape distribution

Figure 6 shows the relationship between the pore size distribution and the pore shape in both environments. The axis ratio is the length of the minor axis divided by the length of the major axis. The lengths of the minor and major axes were determined with the best fitted ellipse. When the axis ratio is 1, the pore shape is spherical. As the axis ratio approaches 0, the pore shape is narrower and longer. As shown in Fig. 6(a), in the terrestrial environment, round shaped pores are mainly distributed in the upper part. In the lower part, small round shaped pores and narrow and long pores are distributed. In the microgravity environment, round shaped pores and narrow and long pores are distributed similarly in both parts of the weld, as shown in Fig. 6(b).

5. DISCUSSION

5.1. Blowhole and wormhole

Pores can be classified into blowholes and wormholes by the difference in the process of formation.

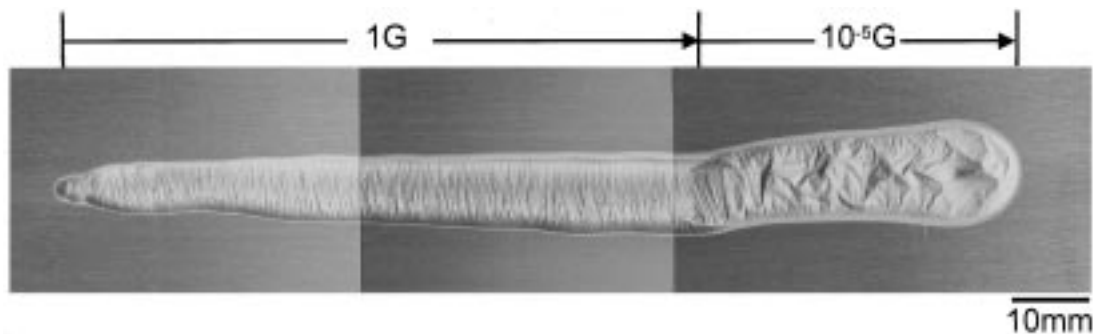


Fig. 2. Typical weld bead appearance of microgravity experiments.

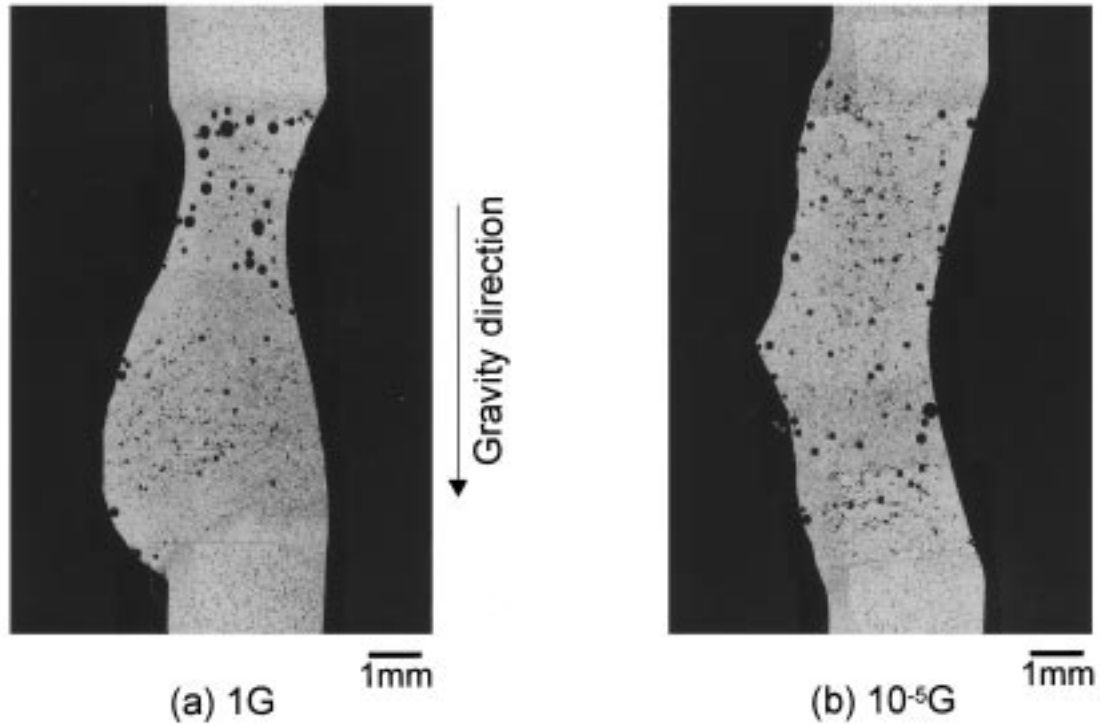


Fig. 3. Transverse sections of bead-on-plate welds in horizontal welding with argon-1% hydrogen mixed shielding gas.

Blowholes are the pores formed while they are surrounded by a liquid phase. Wormholes are the pores formed after or when the surrounding liquid phase is solidified. Therefore, only blowholes can move in the weld and wormholes should stay at the produced points. Accordingly, for an analysis of the behavior of bubbles, blowholes and wormholes

have to be differentiated. Because there is no quantitative definition to differentiate them, in this study an attempt is made to classify them with the shape factor of pores.

Blowholes are spherical because they are formed in a liquid phase. Wormholes, on the other hand, are narrow and long because they are formed at

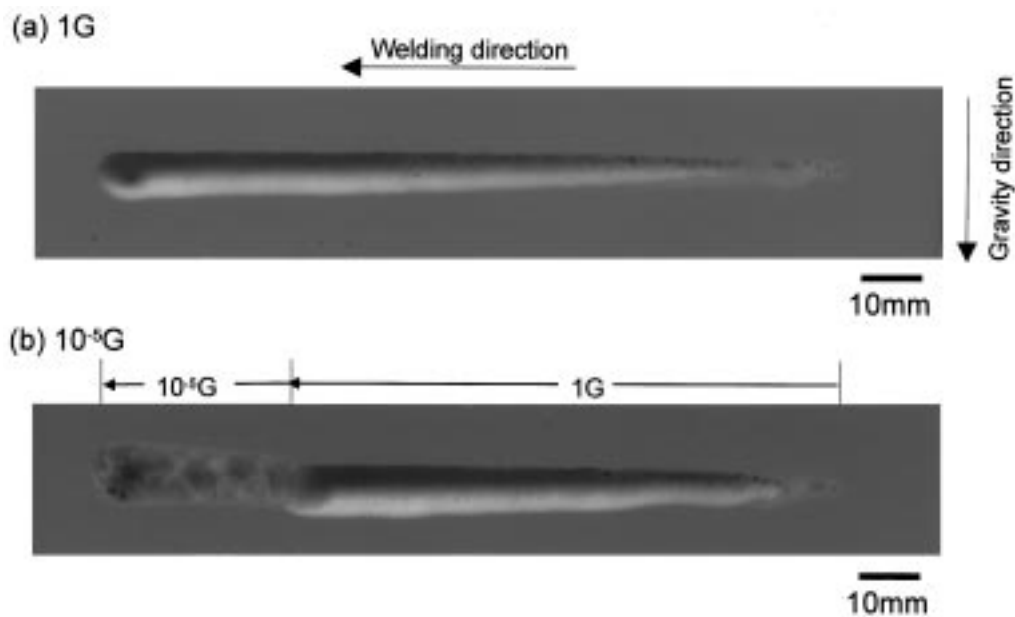


Fig. 4. Radiographs of bead-on-plate welds in horizontal welding with argon-1% hydrogen mixed shielding gas.

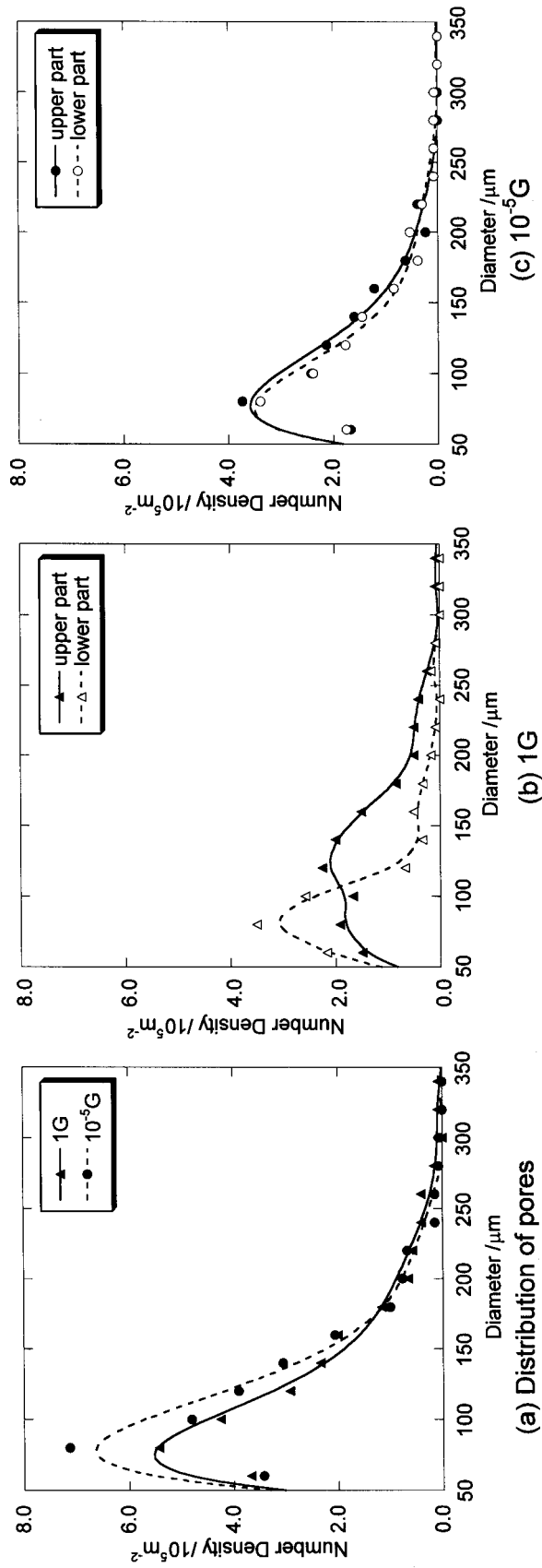


Fig. 5. Pore size distributions observed on transverse sections.

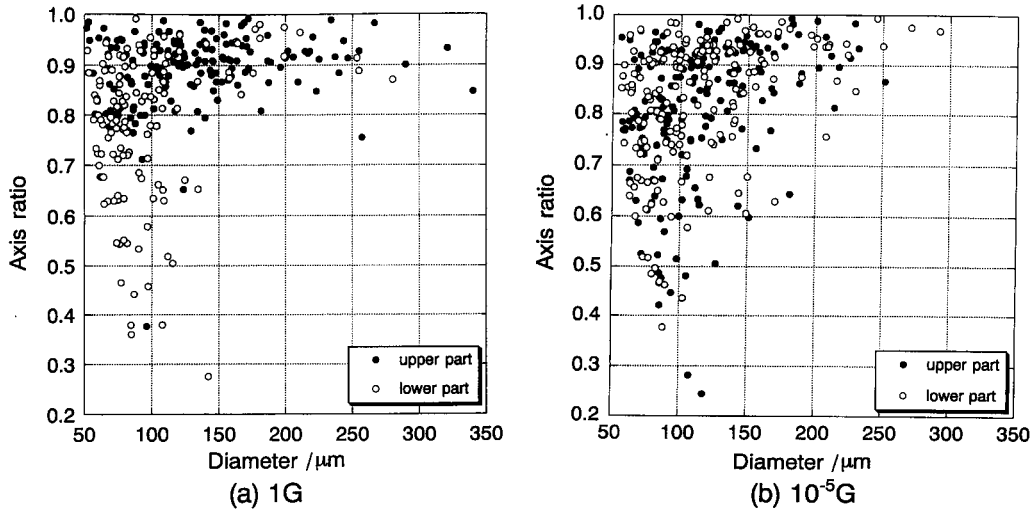


Fig. 6. Relationship between pore size distribution and pore shape.

solid-liquid interfaces. In this study, pores with their axis ratio above 0.75 (longer axis : shorter axis = 4:3) are defined as blowholes and pores with their axis ratio below 0.75 are defined as wormholes from the results of Fig. 6. Under this definition Fig. 7(a) shows the blowhole size distribution, and Fig. 7(b) shows the wormhole size distribution.

The size distribution of blowholes has a peak around $80 \mu\text{m}$ and spread toward the larger size region. On the other hand, the size distribution of wormholes does not spread toward the larger size region and are almost symmetric at the center of around $80 \mu\text{m}$. These results are probably caused by the fact that blowholes combine with other blowholes after their formation and that wormholes do not combine with other wormholes or blowholes. Therefore, these results indicate that a proper separation of blowholes and wormholes is performed in this case because blowholes are formed in a liquid

phase with a chance of combination with other blowholes, and wormholes are formed at a solid-liquid interface without the chance of combination.

The total quantity of wormholes is different between the terrestrial environment and the microgravity environment, as shown in Fig. 7(b). This result indicates that a greater amount of hydrogen is supersaturated in the weld of the terrestrial environment due to a larger cooling rate than that in the microgravity environment.

5.2. Behavior of bubbles

Figures 8(a) and (b) are the separated distributions in the upper part and in the lower part from the results in Fig. 7(a) for both environments, respectively. As shown in Fig. 8(a), in the terrestrial environment, blowholes larger than $135 \mu\text{m}$ ($90 \mu\text{m}$ on the transverse section) were distributed mainly in the upper part. Blowholes smaller than $135 \mu\text{m}$,

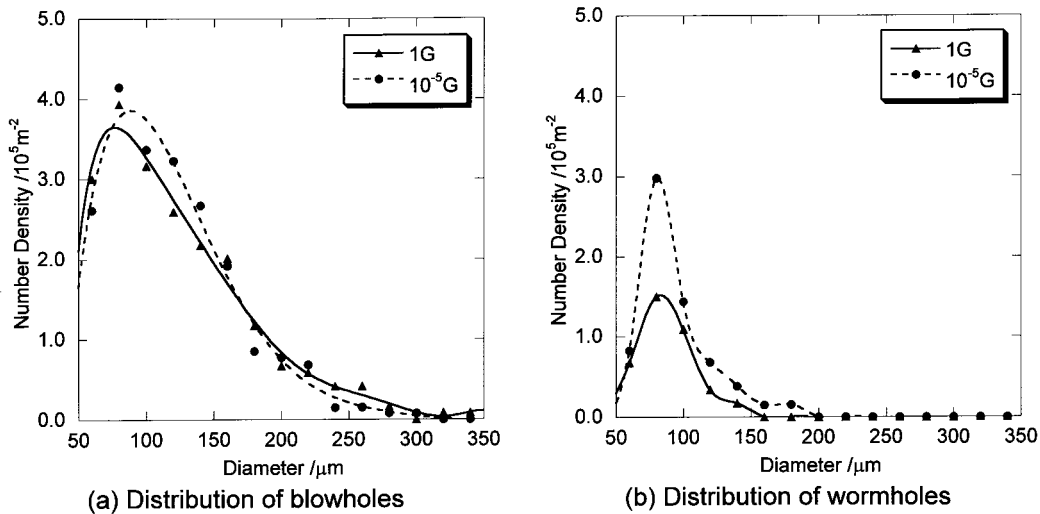


Fig. 7. Blowhole and wormhole size distributions on transverse sections.

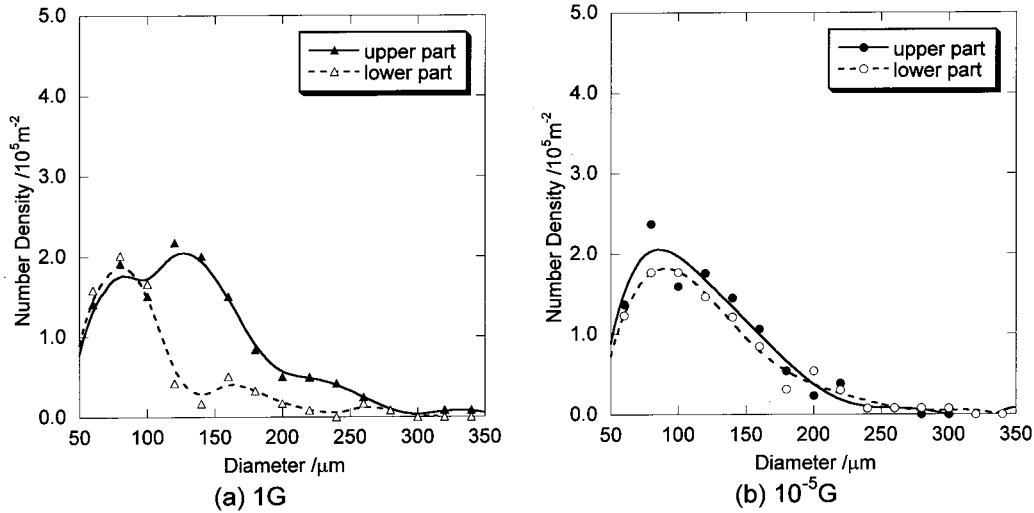


Fig. 8. Blowhole size distributions on transverse sections.

on the other hand, are distributed similarly in both parts. Furthermore, the distribution of the smaller blowholes is very similar to that in the microgravity environment. These results indicate that bubbles smaller than $135\ \mu\text{m}$ are not significantly affected by gravity.

In the microgravity environment, blowholes are distributed similarly in both parts, as shown in Fig. 8(b). Note that the number density of blowholes larger than $135\ \mu\text{m}$ in the microgravity environment is located at the center of the values of the upper part and the lower part in the terrestrial environment. Therefore, unlike our expectation, it should be concluded that in the terrestrial environment, bubbles larger than $135\ \mu\text{m}$ move to the upper part of the molten metal due to buoyancy but that they scarcely combine with other bubbles during the movement. This conclusion agrees with the similar distribution of the total blowholes in both environments, as shown in Fig. 7(a).

As mentioned in Section 5.1, Fig. 7(a) also indicates that a blowhole combines with another blowhole by liquid flow due to various forces such as electromagnetic force, plasma stream, and surface tension. However, they scarcely combine together by the movement due to buoyancy.

The terminal rising velocity, v , of a small, spherical bubble can be estimated by the Stokes law [16]

$$v = \frac{g(\rho_{\text{Me}} - \rho_{\text{H}_2})}{12\mu} d_{\text{H}_2}^2 \quad (Re < 1) \quad (9)$$

where d_{H_2} is the diameter of the bubble, μ is the viscosity of the liquid metal, g is the gravitational acceleration, ρ_{Me} is the density of the liquid metal, ρ_{H_2} is the density of hydrogen, and Re is the Reynolds number. Using this equation, the terminal rising velocity of a hydrogen bubble in a liquid aluminum–4.4% magnesium alloy of the terrestrial environment is estimated as shown in Fig. 9. Because the physical data of the particular liquid

aluminum–magnesium alloy at the particular temperatures cannot be obtained, the physical data are estimated by extrapolating the data of Ref. [17]. In this study, judging from the size of the weld pool and the welding velocity, the duration of the molten state is estimated to be a few seconds. Even when the duration of the molten state is assumed to be 1 s, $70\ \mu\text{m}$ bubbles had enough time to move to the upper part in the duration, as shown in Fig. 9. Therefore, blowholes larger than $70\ \mu\text{m}$ should be mainly distributed in the upper part. However, as shown in Fig. 7(a), the distribution of blowholes smaller than $135\ \mu\text{m}$ is similar in both parts. This is probably because rising of bubbles due to buoyancy is compensated by falling of bubbles with the molten metal drop in the gravity direction.

In the terrestrial environment, when the welding position is performed in a flat position, the volume of pores can be reduced because more bubbles are released from a weld pool than in a horizontal

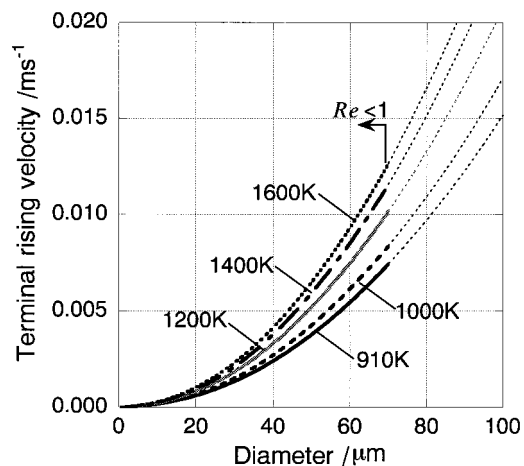


Fig. 9. Estimated terminal rising velocity of hydrogen bubbles in liquid aluminum–4.4% magnesium alloy of terrestrial environment.

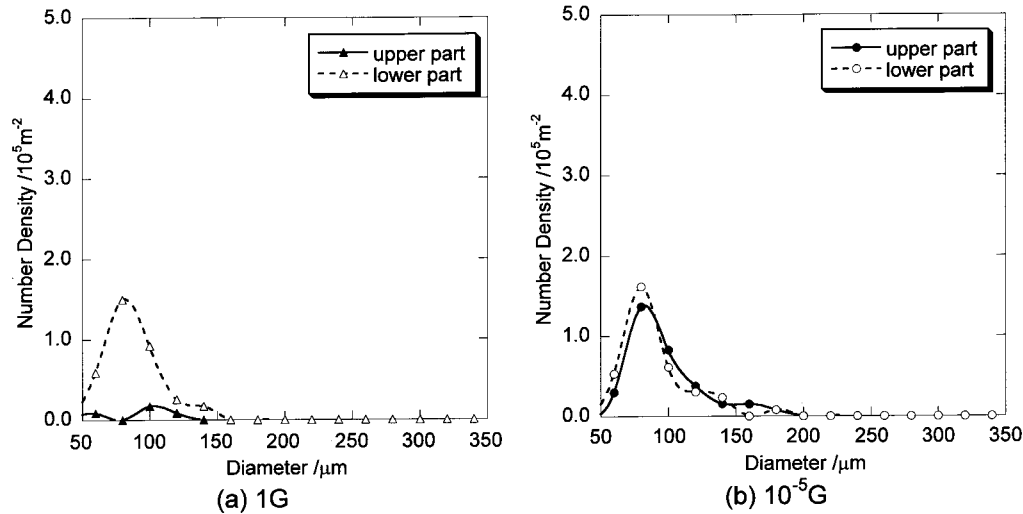


Fig. 10. Wormhole size distributions on transverse sections.

position [18]. However, it would be a problem that in the microgravity environment, bubbles cannot easily be released from the weld pool at any welding position due to the lack of buoyancy. For this problem, stirring of the weld pool may be an effective method. According to Matsuda *et al.* [19], the electromagnetic stirring of the weld pool reduces the formation of pores on earth.

5.3. Analysis of solidification process using pore distribution

As mentioned in Section 5.1, pores can be classified into blowholes and wormholes. When the characteristics of the two types of pores are considered, the solidification process can be estimated as follows. Figures 10(a) and (b) show the separated distributions of wormholes in the upper part and in the lower part of the terrestrial environment and those of the microgravity environment, respectively.

In the terrestrial environment, round shaped pores, that is, blowholes are distributed mainly in the upper part, as shown in Fig. 8(a). Narrow and long pores, that is, wormholes are almost distributed in the lower part, as shown in Fig. 10(a). As mentioned before, blowholes are formed in the liquid phase and wormholes are formed at the solid-liquid interface. This means that blowholes are formed in the early stage of the solidification process, and wormholes are formed at the last stage. It can be judged from these results, the molten metal solidified from the upper part to the lower part, that is, in the gravity direction. In the microgravity environment, on the other hand, blowholes and wormholes are distributed uniformly in both parts, as shown in Figs 8(b) and 10(b). Accordingly, the molten metal is solidified uniformly from both the upper and lower parts.

6. CONCLUSIONS

By welding an aluminum-magnesium alloy 5083 both in a microgravity environment and in a terrestrial environment, the following points were found.

1. Blowholes grow by combining with other blowholes after their formation though wormholes do not combine with other wormholes or blowholes.
2. Gravity does not significantly affect both the movement and the combination of bubbles smaller than 135 μm .
3. Gravity does affect the movement of bubbles larger than 135 μm , though it does not affect the combination of them.
4. It can be judged from the pore size distribution and the pore shape that the molten metal was solidified in the gravity direction in a terrestrial environment and uniformly solidified from both the upper and lower parts in the microgravity environment.

Acknowledgements—The authors greatly appreciate the support of Japan Space Utilization Promotion Center (JSUP) and Japan Microgravity Center (JAMIC).

REFERENCES

1. Paton, B. E., *Weld. Engr*, 1972, **57**, 25.
2. Nance, M. and Jones, J. E., in *A.S.M. Handbook*, Vol. 6, ed. D. L. Olson *et al.* ASM Int., 1993, p. 1020.
3. Nogi, K., Aoki, Y., Fujii, H., Nakata, K. and Kaihara, S., *ISIJ Int.*, 1998, **38**, 163.
4. Daley, D. M., *Weld. J.*, 1960, **39**, 301s.
5. Papritan, J. C. *et al.*, in *Welding Handbook*, Vol. 1, 8th edn, ed. L. P. Connor. AWS, 1987, p. 364.
6. Murphy, J. L., Huber, R. A. and Lever, W. E., *Weld. J.*, 1990, **69**, 125s.
7. Meleka, A. H., *Electron-beam Welding*, 1971, p. 145.
8. Oyler, G. W. and Stout, R. D., *Weld. J.*, 1953, **32**, 457s.

9. Masumoto, I. and Shinoda, T., *Q. J. Jpn. Weld. Soc.*, 1969, **38**, 1075.
10. Itagaki, K., in *Hitetsu Kinzoku Seiren*, ed. Y. Huwa. Jpn. Inst. Metals, 1980, p. 315.
11. Park, S. J., Fujii, H. and Nakae, H., *J. Jpn. Inst. Metals*, 1994, **58**, 208.
12. Packirisamy, S., Schwam, D. and Litt, M. H., *J. Mater. Sci.*, 1995, **30**, 308.
13. Abe, Y., Yasuda, C., Fujiwara, M., Nayama, M. and Okazaki, H., *Mitsubishi Juko Tech. Rev.*, 1990, **27**, 532.
14. Kaihara, S., Kuribayashi, M., Tanji, A., Kawachi, K. and Nezaki, K., *Ishikawajima-Harima Tech. Rev.*, 1994, **34**, 109.
15. Yamaura, Y., *Materia Jpn.*, 1994, **33**, 998.
16. Clift, M., *Bubbles, Drops, and Particles*. Academic Press, New York, 1978, p. 30.
17. Gebhardt, E., Becker, M. and Dorner, S., *Aluminium*, 1955, **31**, 315.
18. Develletian, J. H. and Wood, W. E., *Weld. Res. Council Bull.*, 1983, **290**, 14.
19. Matsuda, F., Nakata, K., Miyanaga, Y., Kayano, T. and Tsukamoto, K., *Trans. JWRI*, 1978, **7**, 181.